Published in final edited form as:

ACS Appl Mater Interfaces. 2018 May 16; 10(19): 16233–16237. doi:10.1021/acsami.7b18855.

Electronic Cortisol Detection Using an Antibody-Embedded Polymer Coupled to a Field-Effect Transistor

Hyun-June Jang[†,‡], **Taein Lee**[†,‡], **Jian Song**[†], **Luisa Russell**[†], **Hui Li**[†], **Jennifer Dailey**[†], **Peter C. Searson**[†], and **Howard E. Katz**[*,†]

[†]Department of Materials Science and Engineering, Johns Hopkins University, 3400 North Charles Street, Baltimore, Maryland 21218-2608, United States

Abstract

A field-effect transistor-based cortisol sensor was demonstrated in physiological conditions. An antibody-embedded polymer on the remote gate was proposed to overcome the Debye length issue (λ_D). The sensing membrane was made by linking poly(styrene-*co*-methacrylic acid) (PSMA) with anticortisol before coating the modified polymer on the remote gate. The embedded receptor in the polymer showed sensitivity from 10 fg/mL to 10 ng/mL for cortisol and a limit of detection (LOD) of 1 pg/mL in 1× PBS where λ_D is 0.2 nm. A LOD of 1 ng/mL was shown in lightly buffered artificial sweat. Finally, a sandwich ELISA confirmed the antibody binding activity of antibody-embedded PSMA.

Graphical abstract

[*]Corresponding Author: hekatz@jhu.edu (H.E.K.).

[‡]**Author Contributions**

These authors made equal contributions to this work.

ORCID

Hui Li: 0000-0002-3826-0735

Peter C. Searson: 0000-0002-5417-0828

Howard E. Katz: 0000-0002-3190-2475

Notes

The authors declare no competing financial interest.

Supporting Information

The Supporting Information is available free of charge on the ACS Publications website at DOI: 10.1021/acsami.7b18855. Experimental details, basic electric characteristics of FET, transfer curve responses (bare PSMA vs cortisol, antisuf PSMA vs cortisol, and antiem PSMA vs 17-α-HPG), transfer-curve responses of antiem PSMA for cortisol in sweat, and ELISA details (PDF)

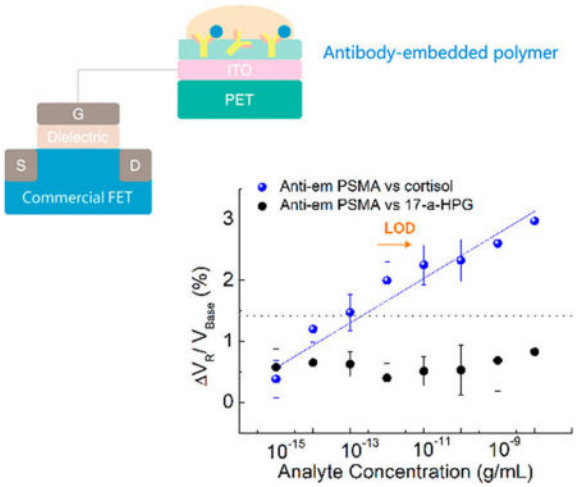

Keywords

cortisol; antibody-embedded polymer; perspiration; Debye screening length; poly(styrene-co-methacrylic acid); transistor biosensor

Physiological stress is considered to be a silent contributor to diverse diseases.[1] Cortisol is a stress biomarker found in sweat, saliva, blood, urine, and interstitial fluid.[2–4] Cortisol sensors based on sweat analysis enable the monitoring of stress levels noninvasively. Reported physiological cortisol levels in human perspiration ranges from 8.16 to 141.7 ng/mL.[5,6] Typical cortisol quantification methods require bulky equipment and several steps in determining cortisol levels.[7,8]

Electrical signaling of the analyte levels by field-effect-transistor (FET) biosensors has scaled down multiple laboratory processes to a portable chip format.[9] A main challenge for the transistor sensors, however, is posed by the Debye screening length (λ_D), arising from the interaction between the sensing surface and electrolyte[10,11] when physical lengths of antibody–antigen complexes are > λ_D associated with physiological media. A common approach to address λ_D is to mix the analyte in body fluid with diluted phosphate-buffered saline (PBS) solution, increasing λ_D.[12] Alternatively, capture-release methods can be applied. In this method, a body fluid is placed on a sensor surface first, resulting in the analyte binding to a surface receptor, after the original solution is replaced with diluted PBS to read the binding signal,[13] complicating the procedure in clinical setups.

There have been many attempts to employ polymers and organic materials to FET sensors because of their intrinsic flexibility and easy fabrication processes.[14–17] A big technical challenge in organic FET (OFET) sensors, however, is instability of the materials under solution-based testing, leading to low sensitivity and selectivity of sensors, compared to inorganic FET sensors.[9] To be specific, water on the dielectrics of OFET biosensors diffuses into the organic semiconducting layer and degrades the innate semiconducting properties. The extended gate (EG) geometry[18] separating the sensing part from the FET transducer is highly desirable for OFET biosensors. This EG geometric not only protects the organic

semiconductor from damage by solution but also harnesses the aforementioned advantages of organic/polymer materials on sensor platforms.[19–21] Alternatively, the OFET transducer can be replaced with inorganic FETs that have much higher stability, while the sensing platform adopts a polymer membrane in the EG geometric in order to avoid any intrinsic instability of OFET such as bias stress effects and signal drifts induced by light.[27]

In this study, we demonstrate label-free detection of cortisol in buffer and artificial perspiration by employing antibody-embedded poly(styrene-*co*-methacrylic acid) (PSMA) sensing gate. The embedded structure of the receptor in the polymer allowed cortisol molecules to bind near the membrane–substrate interface, which overcomes the λ_D issues. Sensitivity for cortisol was obtained in a range from 10 fg/mL to 10 ng/mL with the more rigorous limit of detection (LOD) of 1 pg/mL in 1× PBS. The sensing performance of antibody-embedded PSMA was compared with the performance of the conventional way to functionalize an antibody on the surface of PSMA. We term the antibody-embedded PSMA and antibody-surface-functionalized PSMA as antiem PSMA and antisuf PSMA, respectively. We detected cortisol in lightly buffered artificial sweat with a LOD of 1 ng/mL, and sandwich enzyme-linked immunosorbent assay (ELISA) was performed to confirm the activity of antiem PSMA.

Our measurement system allowed the acquisition of two different electrical signals at the same time from two different sensing gates, as shown in Figures 1a and S1. One of the two sensing gates was monitored as a control setup. Indium–tin oxide (ITO)/poly(ethylene terephthalate) substrate was chosen as the starting material of EG to demonstrate the sensing performance on flexible materials. Any change in the electrical signal on the sensing surface was transmitted to the gate of each FET.[22,23] The transfer curves and output characteristics of a commercial FET were evaluated and are presented in Figure S2 (subthreshold swing, 136 mV/dec; threshold voltage, 1.3 V). Trivial negative drift (−15 uV/min) in the repeated transfer curves was observed from intrinsic FET effects (Figure S3).

The transfer curve had a horizontal shift with increasing pH (Figure 1b), yielding an average sensitivity of 33 mV/pH with a linearity of 97.7% (inset of Figure 1b). Responsive voltages (V_R) were extracted using gate voltages corresponding to a reference drain current (I_R) of 1 μA, and the pH sensitivity was calculated as the slope of the V_R versus pH values. V_R at pH 7 was used as a reference value to calculate ΔV_R in the inset of Figure 1b. Hysteresis was tested by a rapid pH loop of pH 7–4–7–10–7, which showed a reversible tendency with changing pH values (Figure 1c). The difference between the initial and final V_R values of pH 7 was 14 mV.

Shifts in the transfer curve while switching voltages for different concentrations of cortisol indicate the cortisol sensitivity from antisuf PSMA (Figure 2a). Close-up transfer curves are shown in the inset of Figure 2a. No significant hysteresis by double sweeps is observed in the transfer curves. I_R of 1 μA is consistently used to calculate V_R for all of the following plots. The change in V_R was calculated with respect to V_{Base}, where V_{Base} is V_R of the pure 0.05× PBS. Figure 2b shows ΔV_R for cortisol ranging from 1 fg/mL to 10 ng/mL, tested by antisuf PSMA and bare PSMA in diluted 0.05× PBS to increase λ_D. The representative properties of bare PSMA for cortisol are shown in Figure S4. Also, ΔV_R values for 17-α-

hydroxyprogesterone (17-α-HPG), a biochemical precursor of cortisol, are compared in Figure 2b, and typical sensing properties are shown in Figure S5. 17-α-HPG was chosen for our specificity tests because it has a structure and size similar to those of cortisol.[24] The anticortisol and cortisol complexes impose a negative net charge on the sensing membrane. Mean ΔV_R values for experimental samples increase linearly by 0.3% with an R^2 value of 97.5%, ranging from 1 fg/mL to 10 ng/mL. Random signals are observed for two control setups: adding the same cortisol solutions to the sensing gate without any anticortisol surface functionalization and adding the same 17-α-HPG concentrations with antisuf PSMA. The LOD is obtained at the lowest concentration that can be clearly distinguished from a maximum fluctuation by any control sample, which is estimated as 1 pg/mL. No sensitivity for cortisol is shown in repeated tests of experimental samples except in 1× PBS, where λ_D is 0.2 nm. A negative slope is observed for increasing cortisol concentrations (Figures 2c and S6), corresponding to the drift properties of antisuf PSMA (Figure 2d) with PBS solutions (−0.1%/min and −0.3%/min in 1× PBS and 0.05× PBS, respectively). Thus, the sensing ability of a surface-functionalized membrane was limited by λ_D of the media.

A presumed schematic image of the antibody-embedded geometry in the PSMA polymer matrix is depicted in Figure 3a. Representative transfer curves of the FET-coupled antiem PSMA are shown in Figure 3b. Figure 3c demonstrates ΔV_R for cortisol and 17-α-HPG from 1 fg/mL to 10 ng/mL measured by antiem PSMA in 1× PBS. The change in V_R was calculated with respect to V_{Base}, where V_{Base} is V_R of the pure 1× PBS. No definite trend for 17-α-HPG was observed (Figures 3c and S7). In a comparison of the control samples, the sensitivity of antiem PSMA for cortisol in 1× PBS appears from 10 fg/mL and mean ΔV_R values increase linearly by 0.3% with a R^2 value of 94.6%, similar to those of antisuf PSMA, and LOD is estimated as 1 pg/mL. The antibody embedded in the polymer matrix leads to the detection of charge variations much closer to the membrane–substrate interface, reducing the λ_D constraint on the sensing signal. Antiem PSMA had a negative drift (Figure 3d), which is in accordance with the antisuf PSMA result of Figure 2d. The sensitivity of antiem PSMA was maintained up to 1.7 days at 4 °C, with a large standard deviation. However, the device sensitivity degraded after 2 days or more and showed random signals with lower R^2, corresponding to the previously described nonresponsive control experiments.

pH values in human sweat vary from pH 2 to 8.2.[25] Therefore, pH 7.4 of the artificial sweat was chosen for our sweat tests in compliance with the conditions performed above. 10% 1× PBS was added to the artificial sweat as a buffer against changing the pH of the media to avoid any interference of the signal from background media pH.[26,27] While reproducible detection of cortisol in artificial sweat apparently requires greater sample quality control than that from simple buffers, five samples out of a total of eight showed a linear response for cortisol in artificial sweat with pH 7.4, in a range from 1 fg/mL to 100 μg/mL (Figures 3f and S8). The approximated LOD considering the maximum fluctuation in Figure 3c is 1 ng/mL. The change in V_R was calculated with respect to V_{Base} of artificial sweat including 10% 1× PBS. ΔV_R increases by 0.2% for every 10-fold increase in the cortisol concentration, which is smaller than those shown in the PBS solution. One possible reason is that sweat has more salts, and the resulting Debye screening effect would be exponentially larger.

It is noted that the yield to show sensitivity is highly reduced for pure artificial sweat tests without adding 10% 1× PBS (two samples out of a total of eight), as shown in Figure S9. In the same context, none of the samples in sweat with pH 4.5 showed sensitivity even after they were diluted by 1× PBS to 5% and 10% because it was still not in the controlled pH regime of background media (Figure S10). The sensing mechanism of FET biosensors based on varying isoelectric points causes pH levels to fluctuate in the media, often leading to a different charge distribution on the surface even though the sensors detect the same analyte.[12] This leads to a situation where the various pH levels have different or no sensitivity for the same biomarker, which is another major challenge in clinical applications of FET biosensors aside from λ_D issues.[26,27] Capture–release methods mentioned in the introduction can address this issue. Another way is to highly dilute physiological sweat with a reference buffer solution to reach the controlled pH regime. In this case, a higher sensing capacity would be required to detect lower cortisol concentrations in the highly diluted solution. Detecting analyte in physiological sweat is still challenging, but our antiem PSMA shows a way to overcome λ_D constraints.

To observe the specific binding on our platform more directly, a standard sandwich ELISA procedure was conducted using fluorescein isothiocyanate (FITC)-conjugated antibodies on antisuf PSMA (Figure 4a). Higher fluorescence intensity (FI) was observed for the standard sandwich ELISA with an antibody–antigen–fluorescein complex. However, lower FI was shown for the control samples with a sandwich ELISA excluding cortisol and primary antibody. Similarly, a standard sandwich ELISA with an antiem PSMA–antigen–fluorescein complex (Figure 4b) showed higher FI than those of control samples excluding cortisol and replacing cortisol with 17-α HPG for selectivity testing. This confirms that there is significant specificity of binding and that the anticortisol protein remains active in antiem PSMA although the orientation of the antibody inside the PSMA polymer may be random. We estimated that around 1.5% of the antibodies added to the antiem PSMA mixture was active based on the ELISA data (Figure S11). While nonspecific binding was also observed, this is in a step that is not part of the electronic sensing procedure.

We demonstrated the electrical detection of cortisol using polymers on a remote flexible gate platform coupled with a commercial FET that is highly sensitive, specific, and disposable. To the best of our knowledge, this is the first demonstration of FET-based cortisol sensing. Antiem PSMA showed the sensitivity from 10 fg/mL to 10 ng/mL in 1× PBS, while clear selectivity was shown from 1 pg/mL. In our sweat tests, antiem PSMA showed the potential to overcome the λ_D constraint showing a LOD of 1 ng/mL in lightly buffered artificial sweat. The specificity of antiem PSMA was also demonstrated by ELISA. This technique increases the possibility of detecting cortisol in saliva or sweat using transistor biosensors in clinical settings.

Supplementary Material

Refer to Web version on PubMed Central for supplementary material.

Acknowledgments

We thank Dr. Olivia Alley for insightful comments and a critical reading of the manuscript. The authors appreciate Suchang Mun's graphical artwork. The pH and cortisol sensing tests were funded by the Air Force Research Laboratory via a subcontract with the Nano Terra Corporation. The development of the remote gate device architecture and the ELISA study were funded by the National Institute of Biomedical Imaging and Bioengineering of the National Institutes of Health under Award R21EB018426. The content is solely the responsibility of the authors and does not necessarily represent the official views of the National Institutes of Health.

References

1. Rozanski A, Blumenthal JA, Kaplan J. Impact of psychological factors on the pathogenesis of cardiovascular disease and implications for therapy. Circulation. 1999; 99:2192–2217. [PubMed: 10217662]
2. Munje RD, Muthukumar S, Panneer Selvam A, Prasad S. Flexible nanoporous tunable electrical double layer biosensors for sweat diagnostics. Sci Rep. 2015; 5:14586. [PubMed: 26420511]
3. Stevens RC, Soelberg SD, Near S, Furlong CE. Detection of cortisol in saliva with a flow-filtered, portable surface plasmon resonance biosensor system. Anal Chem. 2008; 80:6747–6751. [PubMed: 18656950]
4. Kumar A, Aravamudhan S, Gordic M, Bhansali S, Mohapatra SS. Ultrasensitive detection of cortisol with enzyme fragment complementation technology using functionalized nanowire. Biosens Bioelectron. 2007; 22:2138–2144. [PubMed: 17097283]
5. Kinnamon D, Ghanta R, Lin KC, Muthukumar S, Prasad S. Portable biosensor for monitoring cortisol in low-volume perspired human sweat. Sci Rep. 2017; 7:13312. [PubMed: 29042582]
6. Russell E, Koren G, Rieder M, Van Uum SH. The detection of cortisol in human sweat: implications for measurement of cortisol in hair. Ther Drug Monit. 2014; 36:30–34. [PubMed: 24216536]
7. Kaushik A, Vasudev A, Arya SK, Pasha SK, Bhansali S. Recent advances in cortisol sensing technologies for point-of-care application. Biosens Bioelectron. 2014; 53:499–512. [PubMed: 24212052]
8. Singh A, Kaushik A, Kumar R, Nair M, Bhansali S. Electrochemical sensing of cortisol: a recent update. Appl Biochem Biotechnol. 2014; 174:1115–1126. [PubMed: 24723204]
9. Huang WG, Besar K, LeCover R, Dulloor P, Sinha J, MArtinez Hardigree JF, Pick C, Swavola J, Everett AD, Frechette J, Bevan M, Katz HE. Label-free brain injury biomarker detection based on highly sensitive large area organic thin film transistor with hybrid coupling layer. Chem Sci. 2014; 5:416–426.
10. Jang HJ, Ahn J, Kim MG, Shin YB, Jeun M, Cho WJ, Lee KH. Electrical signaling of enzyme-linked immunosorbent assays with an ion-sensitive field-effect transistor. Biosens Bioelectron. 2015; 64:318–323. [PubMed: 25240958]
11. Stern E, Wagner R, Sigworth FJ, Breaker R, Fahmy TM, Reed MA. Importance of the debye screening length on nanowire field effect transistor sensors. Nano Lett. 2007; 7:3405–3409. [PubMed: 17914853]
12. Makowski MS, Ivanisevic A. Molecular Analysis of Blood with Micro-/Nanoscale Field-Effect-Transistor Biosensors. Small. 2011; 7:1863–1875. [PubMed: 21638783]
13. Stern E, Vacic A, Rajan NK, Criscione JM, Park J, Ilic BR, Mooney DJ, Reed MA, Fahmy TM. Label-free biomarker detection from whole blood. Nat Nanotechnol. 2010; 5:138–142. [PubMed: 20010825]
14. Lai S, Demelas M, Casula G, Cosseddu P, Barbaro M, Bonfiglio A. Ultralow voltage, OTFT-based sensor for label-free DNA detection. Adv Mater. 2013; 25:103–107. [PubMed: 23027594]
15. Zang YP, Zhang FJ, Huang DZ, Di CA, Zhu DB. Sensitive Flexible Magnetic Sensors using Organic Transistors with Magnetic-Functionalized Suspended Gate Electrodes. Adv Mater. 2015; 27:7979–7985. [PubMed: 26523840]
16. Minami T, Sasaki Y, Minamiki T, Wakida S, Kurita R, Niwa O, Tokito S. Selective nitrate detection by an enzymatic sensor based on an extended-gate type organic field-effect transistor. Biosens Bioelectron. 2016; 81:87–91. [PubMed: 26921557]

17. Magliulo M, Mallardi A, Mulla MY, Cotrone S, Pistillo BR, Favia P, Vikholm-Lundin I, Palazzo G, Torsi L. Electrolyte-Gated Organic Field-Effect Transistor Sensors Based on Supported Biotinylated Phospholipid Bilayer. Adv Mater. 2013; 25:2090–2094. [PubMed: 23288589]
18. Guan W, Duan X, Reed MA. Highly specific and sensitive non-enzymatic determination of uric acid in serum and urine by extended gate field effect transistor sensors. Biosens Bioelectron. 2014; 51:225–231. [PubMed: 23968728]
19. Song J, Dailey J, Li H, Jang HJ, Zhang PF, Wang JTH, Everett AD, Katz HE. Extended Solution Gate OFET-Based Biosensor for Label-Free Glial Fibrillary Acidic Protein Detection with Polyethylene Glycol-Containing Bioreceptor Layer. Adv Funct Mater. 2017; 27:1606506. [PubMed: 29606930]
20. Zhang L, Wang G, Wu D, Xiong C, Zheng L, Ding Y, Lu H, Zhang G, Qiu L. Highly selective and sensitive sensor based on an organic electrochemical transistor for the detection of ascorbic acid. Biosens Bioelectron. 2018; 100:235–241. [PubMed: 28923558]
21. Minami T, Minamiki T, Hashima Y, Yokoyama D, Sekine T, Fukuda K, Kumaki D, Tokito S. An extended-gate type organic field effect transistor functionalised by phenylboronic acid for saccharide detection in water. Chem Commun. 2014; 50:15613–15615.
22. Jang HJ, Gu JG, Cho WJ. Sensitivity enhancement of amorphous InGaZnO thin film transistor based extended gate field-effect transistors with dual-gate operation. Sens Actuators, B. 2013; 181:880–884.
23. Lee IK, Jeun M, Jang HJ, Cho WJ, Lee KH. A self-amplified transistor immunosensor under dual gate operation: highly sensitive detection of hepatitis B surface antigen. Nanoscale. 2015; 7:16789–16797. [PubMed: 26399739]
24. Honour JW. 17-Hydroxyprogesterone in children, adolescents and adults. Ann Clin Biochem. 2014; 51:424–440. [PubMed: 24711560]
25. Harvey CJ, LeBouf RF, Stefaniak AB. Formulation and stability of a novel artificial human sweat under conditions of storage and use. Toxicol In Vitro. 2010; 24:1790–1796. [PubMed: 20599493]
26. Hammock ML, Knopfmacher O, Naab BD, Tok JBH, Bao ZA. Investigation of Protein Detection Parameters Using Nanofunctionalized Organic Field-Effect Transistors. ACS Nano. 2013; 7:3970–3980. [PubMed: 23597051]
27. Khan HU, Jang J, Kim JJ, Knoll W. Situ Antibody Detection and Charge Discrimination Using Aqueous Stable Pentacene Transistor Biosensors. J Am Chem Soc. 2011; 133:2170–2176. [PubMed: 21280621]

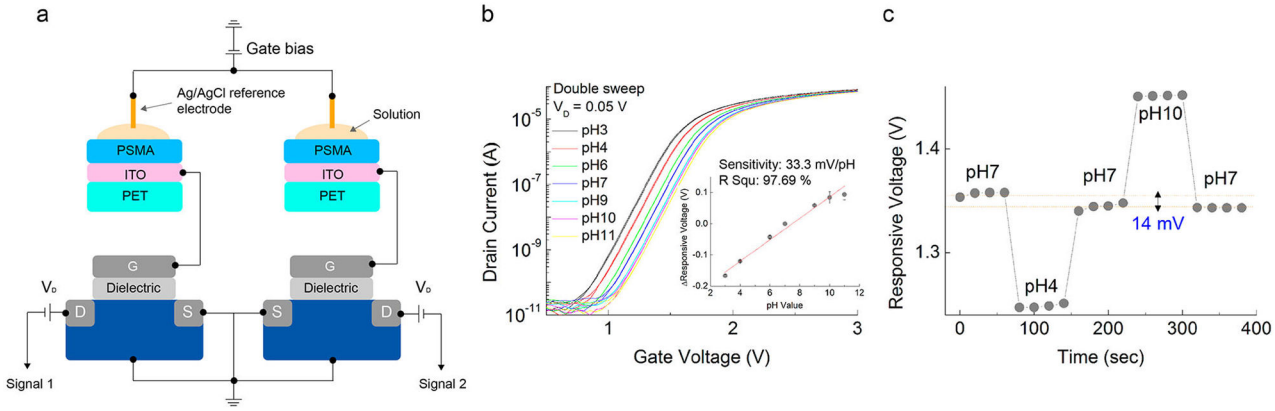

Figure 1.

(a) Schematic image of the measurement system. Two different remote sensing gates were coupled to the gate of each commercial FET. (b) Representative transfer curves of FET with the remote PSMA membrane with changing pH values. The inset figure shows ΔV_R versus pH values from an aggregate of five transfer curves. (c) Hysteresis measured through a pH loop of pH 7–4–7–10–7.

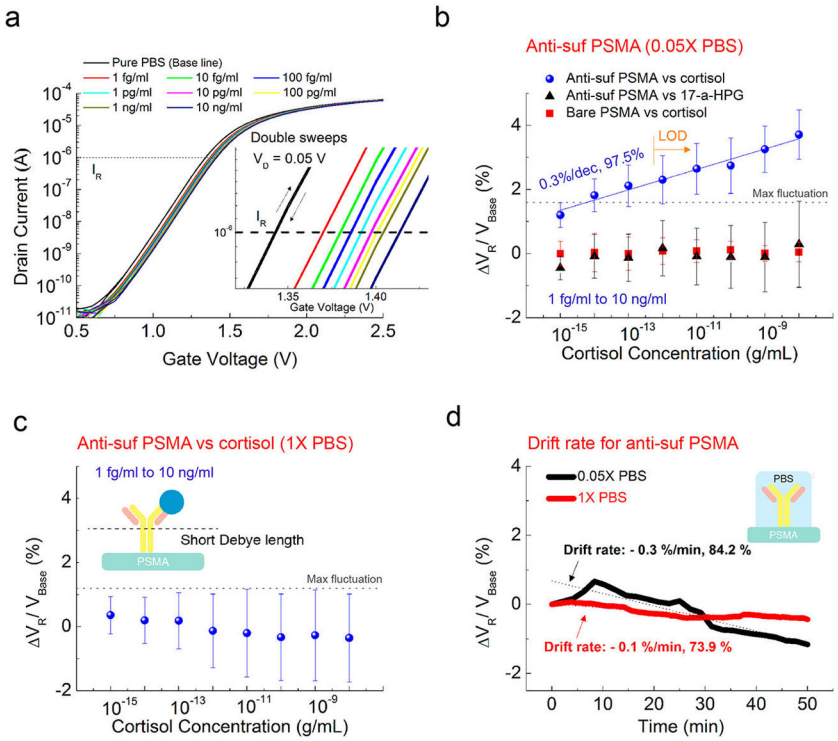

Figure 2.

(a) Representative transfer curves of antisuf PSMA versus cortisol concentration in 0.05× PBS. Inset: Close-up transfer curves. (b) ΔV_R response of antisuf PSMA in terms of cortisol and 17-α-HPG concentrations in 0.05× PBS. The ΔV_R response of cortisol on bare PSMA is compared. Mean ΔV_R increase by 0.3% for every 10-fold increase in the cortisol concentration for five samples. Random signals for cortisol were observed in the bare PSMA for four samples. Also, no sensitivity for 17-α-HPG is obtained by antisuf PSMA for three samples. (c) ΔV_R of antisuf PSMA versus different concentrations of cortisol in a 1× PBS solution over three samples. (d) Drift rate of antisuf PSMA measured in 1× and 0.05× PBS by repeating the transfer curve for 50 min after stabilization. In both cases, the drift had a negative slope.

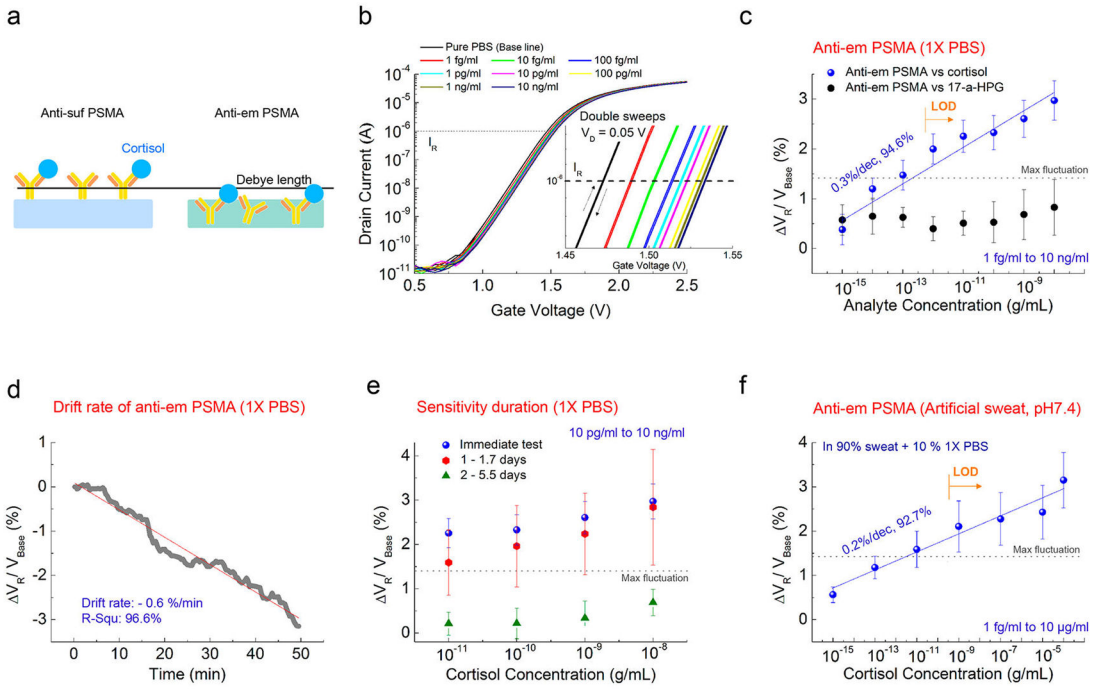

Figure 3.

(a) Presumed schematic image of antibody-embedded geometric in the PSMA polymer matrix. (b) Representative transfer curves of antiem PSMA versus cortisol concentration in 1× PBS. Inset: Close-up transfer curves. (c) ΔV_R response of antiem PSMA in terms of the cortisol and 17-α-HPG concentration V_R in a 1× PBS solution. ΔV_R increases by 0.3% with increasing cortisol over eight samples of antiem PSMA. Random signal in terms of 17-α-HPG over four samples of antiem PSMA. (d) Drift properties of antiem PSMA in 1× PBS over 50 min after stabilization. A negative slope was obtained like that of Figure 2d. (e) Cortisol sensitivity of antiem PSMA as a function of days stored, in a range of cortisol from 10 pg/mL to 10 ng/mL (10 and 6 samples for immediate and stored samples, respectively). Random signals appeared for six samples 2 days after storage. (f) Cortisol sensitivity of antiem PSMA in artificial sweat with pH 7.4 in a range from 1 fg/mL to 100 μg/mL for five samples. 10% 1× PBS was added to the artificial sweat. Three other samples gave little or no response.

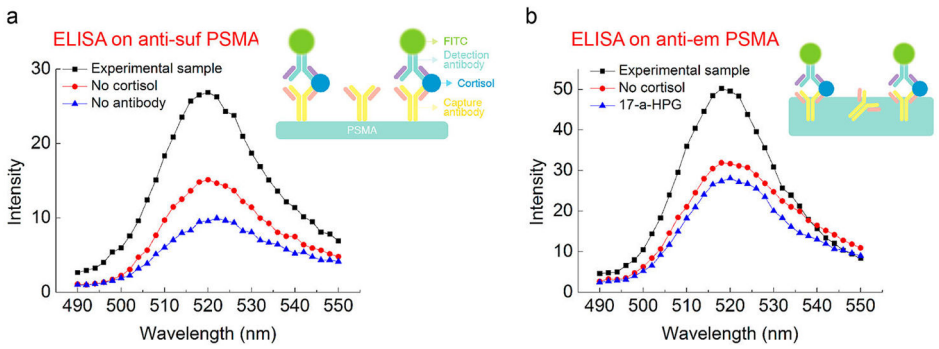

Figure 4.

(a) FI of FITC-labeled antisuf PSMA via standard ELISA. Control setups without the addition of cortisol and without the addition of a primary antibody from procedures in step 4a were compared. (b) FI of FITC-labeled antiem PSMA. Control setups without the addition of cortisol and adding 17-α HPG instead of cortisol from procedures in step 4b were compared.